International Journal of Pharmaceutics 416 (2011) 314–322

Contents lists available at ScienceDirect

International Journal of Pharmaceutics

journal homepage: www.elsevier.com/locate/ijpharm

Pharmaceutical Nanotechnology

Targeted delivery of a poorly water-soluble compound to hair follicles using polymeric nanoparticle suspensions

Michael Morgen[a], Guang Wei Lu[b,*], Daniel Du[b,1], Randall Stehle[b,2], Franz Lembke[a], Jessica Cervantes[a], Susan Ciotti[b,3], Roy Haskell[b,4], Dan Smithey[a,5], Kevin Haley[a,6], Conglin Fan[c]

[a] Bend Research Inc., 64550 Research Road, Bend, OR 97701, USA
[b] Pfizer Worldwide Research and Development, Eastern Point Road, Groton, CT 06340, USA
[c] Pfizer Worldwide Research and Development, 10724 Science Center Drive, San Diego, CA 92121, USA

ARTICLE INFO

Article history:
Received 4 April 2011
Received in revised form 30 May 2011
Accepted 12 June 2011
Available online 21 June 2011

Keywords:
Nanoparticles
Dermal
Low solubility
Hair follicles

ABSTRACT

This study explored the utility of topically applied polymeric nanoparticle suspensions to target delivery of poorly water-soluble drugs to hair follicles. Several formulations of amorphous drug/polymer nanoparticles were prepared from ethyl cellulose and UK-157,147 (systematic name (3S,4R)-[6-(3-hydroxyphenyl)sulfonyl]-2,2,3-trimethyl-4-(2-methyl-3-oxo-2,3-dihydropyridazin-6-yloxy)-3-chromanol), a potassium channel opener, using sodium glycocholate (NaGC) as a surface stabilizer. Nanoparticle suspensions were evaluated to determine if targeted drug delivery to sebaceous glands and hair follicles could be achieved. In *in vitro* testing with rabbit ear tissue, delivery of UK-157,147 to the follicles was demonstrated with limited distribution to the surrounding dermis. Delivery to hair follicles was also demonstrated *in vivo*, based on stimulation of hair growth in tests of 100-nm nanoparticles with a C3H mouse model. The nanoparticles were well-tolerated, with no visible skin irritation. *In vivo* tests of smaller nanoparticles with a hamster ear model also indicated targeted delivery to sebaceous glands. The nanoparticles released drug rapidly in *in vitro* nonsink dissolution tests and were stable in suspension for 3 months.

The present results show selective drug delivery to the follicle by follicular transport of nanoparticles and rapid release of a poorly water-soluble drug. Thus, nanoparticles represent a promising approach for targeted topical delivery of low-solubility compounds to hair follicles.

1. Introduction

Nanoparticles represent an attractive means to achieve preferential delivery of therapeutic agents to target tissues in the human body, achieving the desired drug release profile at the site without the use of organic solvents (Moghimi et al., 2001; Yih and Al-Fandi, 2006). Nanoparticles have been successfully used to target drug delivery, improve bioavailability, sustain drug release, and increase dissolved drug levels for poorly water-soluble compounds (Singh and Lillard, 2009).

This article describes the results of studies to investigate the feasibility of using suspensions containing drug/polymer nanoparticles to achieve targeted delivery to hair follicles of UK-157,147 (systematic name (3S,4R)-[6-(3-hydroxyphenyl)sulfonyl]-2,2,3-trimethyl-4-(2-methyl-3-oxo-2,3-dihydropyridazin-6-yloxy)-3-chromanol), a potassium channel opener with low aqueous solubility. The structure of this compound is shown in Fig. 1.

Successful drug targeting requires increasing the proportion of drug delivered to the target tissue relative to the systemic exposure (Knorr et al., 2009). For treatment of some dermatological indications, this requires delivering a higher proportion of drug to the hair follicles and sebaceous glands. Restricting the amount of drug travelling through the transepidermal pathway to systemic circulation can be important for increasing the drug's therapeutic index, particularly for drugs that require chronic use or drugs that produce significant adverse events in other locations within the body. For example, severe side effects occur when podophyllotoxin is absorbed systemically, but no such effects occur when

Abbreviations: D_{fr}, dissolved free drug; D_p, drug in nanoparticle; K_p, polymer/aqueous partition coefficient; V_p, volume fraction of ethyl cellulose in the suspension.

* Corresponding author. Tel.: +1 860 686 1598; fax: +1 860 686 7810.
E-mail address: guang.w.lu@pfizer.com (G.W. Lu).
[1] Current address: GlaxoSmithKline, Medical Affairs, 1500 Littleton Road, Parsippany, NJ 07054, USA.
[2] Current address: 5886 West Q Avenue, Kalamazoo, MI 49009, USA.
[3] Current address: NanoBio Corp., 2311 Green Road, Suite A, Ann Arbor, MI 48105, USA.
[4] Current address: Bristol-Myers Squibb Co., Discovery Pharmaceutics, 5 Research Parkway, Wallingford, CT 06492, USA.
[5] Current address: Agere Pharmaceuticals, 62925 NE 18th Street, Bend, OR 97701, USA.
[6] Current address: 16651 Stage Stop Drive, Bend, OR 97707, USA.

0378-5173/$ – see front matter © 2011 Elsevier B.V. All rights reserved.
doi:10.1016/j.ijpharm.2011.06.019

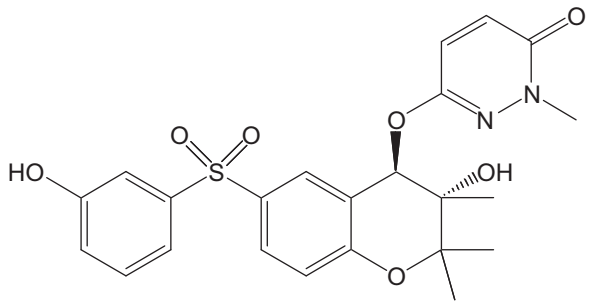

Fig. 1. Chemical structure of UK-157,147 (systematic name (3S,4R)-[6-(3-hydroxyphenyl)sulfonyl]-2,2,3-trimethyl-4-(2-methyl-3-oxo-2,3-dihydropyridazin-6-yloxy)-3-chromanol).

~75-nm solid lipid nanoparticles containing podophyllotoxin are delivered with epidermal targeting (Chen et al., 2006).

In principle, topically applied agents can reach the lower portion of the hair follicles by either the transfollicular or the transepidermal route. The former pathway involves drug diffusion through the upper reaches of the pilosebaceous gland, whereas the latter pathway involves secondary local/systemic distribution into hair follicles. The relative importance of the two routes depends on the drug and the formulation.

In many cases, delivery occurs simultaneously via both transepidermal and transfollicular pathways. For example, caffeine appears in systemic circulation within 5 min after it is topically applied as a solution, but takes 20 min to appear if the same formulation is applied to skin in which the hair follicles are blocked. These results demonstrate the importance of the transfollicular route (Otberg et al., 2008).

Significant research has been focused on drug transport via the transfollicular route using various topical dosage forms (Rolland et al., 1993; Lademann et al., 2005; Jung et al., 2006; Chourasia and Jain, 2009). Many different nanoparticle systems, including those based on metal oxides (Lekki et al., 2007), liposomes (Jung et al., 2006), and polymeric materials (Shim et al., 2004; Alvarez-Roman et al., 2004; Tsujimoto et al., 2007) have been investigated for use as follicular drug-delivery carriers.

Several studies have demonstrated that nanoparticles can reach the deep hair follicles after topical application to human and animal skin, with some research suggesting that follicular delivery is more efficient with smaller nanoparticles—generally, those less than about 300 nm in diameter—than larger nanoparticles (Chen et al., 2006; Shim et al., 2004; Alvarez-Roman et al., 2004; Vogt et al., 2006). For example, Vogt et al. (2006) found that 40-nm nanoparticles were internalized by Langerhans cells found around hair follicles of human skin, but 750-nm and 1500-nm nanoparticles were not.

Lademann et al. (2005) clearly showed the penetration of 320-nm poly(lactide-co-glycolide) (PLGA) nanoparticles into hair follicles in porcine and human skin. With massage after topical application, the nanoparticles penetrated much deeper and remained in the hair follicles much longer than a formulation that did not contain nanoparticles (Lademann et al., 2007). Similarly, Rancan et al. (2009) reported that 228-nm and 365-nm polylactic acid (PLA) nanoparticles penetrated human hair follicles and released loaded dyes into the surrounding tissues, indicating the potential of targeted drug delivery using nanoparticle systems.

Although biodegradable and nonbiodegradable nanoparticles have been reported, biodegradability may not be essential, because it is likely nanoparticles will be eliminated from the skin surface (e.g., due to hair growth, outflow of sebum, and epidermal turnover). In addition, evidence exists that nanoparticles larger than 100 nm do not pass out of the follicles into living tissue (Lademann et al., 2007). Another study suggests that polymeric nanoparticles ranging in size from approximately 30 to 100 nm did not penetrate beyond the superficial stratum corneum (Wu et al., 2009). One study showed 20-nm titanium oxide nanoparticles penetrated 400 μm into the hair follicles, but no evidence of nanoparticles in vital tissue or sebaceous glands was observed (Lekki et al., 2007).

On the other hand, a recent study in mice suggested that 40- and 200-nm polystyrene nanoparticles taken up into hair diffused into the surrounding tissue and were transported to the draining lymph nodes (Mahe et al., 2009). Additional studies would be valuable to assess the potential for transport of nanoparticles into surrounding tissue from hair follicles.

In this study, we investigated the feasibility of using a suspension of drug/polymer nanoparticles to achieve targeted delivery of UK-157,147, a low-solubility compound, to hair follicles. For this study, ethyl cellulose—which is known to solubilize a large number of hydrophobic drugs—was chosen as the matrix for the UK-157,147 nanoparticles. (It is likely that similar solubilization can be achieved using other polymeric materials, including biodegradable polymers if desired.)

The nanoparticles were characterized, and their performance was evaluated in (1) an *in vitro* test to evaluate drug distribution within the skin (using rabbit ear tissue); (2) an *in vivo* test to evaluate drug delivery to sebaceous glands (using a Golden Syrian hamster ear model); and (3) an *in vivo* test to evaluate hair-growth efficacy (using a C3H mouse model).

In this study, delivery of UK-157,147 was demonstrated to the sebaceous glands in a hamster ear model using an aqueous nanoparticle suspension. Similar formulations with larger nanoparticles also stimulated hair growth in the C3H mouse model, caused no visible skin irritation and were well-tolerated. *In vitro* imaging of rabbit ear tissue suggests that aqueous nanoparticle suspensions successfully limit distribution of small-molecule drugs to the dermis while delivering drug to the follicles.

These results suggest that nanoparticle suspensions can effectively deliver low-molecular-weight drugs to the follicles through the transfollicular route, while limiting distribution to the rest of the skin and to systemic circulation. By targeting delivery to the hair follicles, nanoparticles have the potential to improve the therapeutic index for a number of topically applied drugs.

2. Materials and methods

2.1. Materials

UK-157,147 was provided by Pfizer Inc. (Groton, CT). Ethyl cellulose (Ethocel® Viscosity 4) was a generous gift from the Dow Chemical Co. (Midland, MI). Sodium glycocholate (NaGC) (Product No. G7132), poly[methyl methacrylate-co-(fluorecein-o-methacrylate)] (PMMA)(Product No. 56,888-0), and poly[2-methoxy-b-(2-ethylhexyloxy)-1,4-phenylenevinylene] (MEH-PPV) (Product No. 541435) were purchased from Sigma Aldrich Corp. (St. Louis, MO). Methylene chloride (Product No. BDH1113) was purchased from VWR International LLC (Radnor, PA). Syringe filters (1-μm glass-microfiber membrane and 0.2-μm polyethersulfone [PES] Supor filters) were purchased from Pall Corp. (Port Washington, NY). Molecular-weight-cutoff (MWCO) filters (100 kDa, Microcon Ultracel YM-100) were purchased from Millipore Corp. (Billerica, MA).

2.2. Nanoparticle preparation methods

For the *in vitro* tests to evaluate distribution within the skin using rabbit ear tissue, 19:1:0.6 ethyl cellulose: MEH-PPV:NaGC

nanoparticles were prepared by dissolving (1) 594 mg of ethyl cellulose and 31 mg of MEH-PPV in 5 ml of methylene chloride; and (2) 19 mg of NaGC in 20 ml of water. The methylene chloride solution containing dissolved polymers and drug was mixed with the NaGC solution using a rotor stator (Polytron 3100, Kinematica Inc., Bohemia, NY) at 10,000 rpm for 3 min. This coarse emulsion was further emulsified at 12,500 psi for 6 min using a microfluidizer (Microfluidics M110S, Newton, MA) fitted with a Z-shaped interaction chamber with a 100-μm-diameter channel. The emulsion was then placed on a rotoevaporator, where the methylene chloride was removed under reduced pressure at approximately 25 °C. The resulting aqueous suspension was filtered through a 1-μm glass-microfiber syringe filter and potency was measured using the method described below.

A placebo second nanoparticle suspension, in which Nile Red dye was incorporated into nanoparticles, was made using the emulsion process described above. For these nanoparticles, solutions that were prepared by dissolving 1200 mg of ethyl cellulose and 12 mg of Nile Red in 9 ml of methylene chloride, while 20 mg of NaGC was dissolved in 20 ml of Milli-Q™ water, yielding 10:0.1:0.17 ethyl cellulose:Nile Red:NaGC nanoparticles.

An organic solution to evaluate drug distribution within the skin *in vitro* using a rabbit ear model was made by dissolving Nile Red dye in 60:20:20 ethanol:propylene glycol:isopropyl myristate, which is a typical vehicle used for topical drug delivery. The solution was made by mixing 6 ml of ethanol, 2 ml of propylene glycol, and 2 ml of isopropyl myristate, and then adding 10 mg of Nile Red.

For the study to evaluate drug delivery to sebaceous glands *in vivo* using a Golden Syrian hamster ear model, 1:3:2 UK-157,147:ethyl cellulose:NaGC/PMMA fluorescent nanoparticles were made by emulsion. Solutions were prepared by dissolving (1) 400 mg of UK-157,147, 1.2 g of ethyl cellulose, and 80 mg of PMMA in 9 ml of methylene chloride; and (2) 800 mg of NaGC in 20 ml of Milli-Q water. The two solutions were mixed and the nanoparticles were made using an emulsion procedure similar to the one described above. The suspension was filtered through a 1-μm glass-microfiber syringe filter. Potency was measured using the method described below, and the suspension was then diluted to 10 mg active per ml (mg A/ml).

For the *in vivo* hair-growth efficacy tests in the C3H mouse model, 1:3:0.06 UK-157,147:ethyl cellulose:NaGC nanoparticles were prepared. The amount of surfactant (i.e., NaGC) was reduced relative to that used in the hamster model to minimize the potential for skin irritation during a longer study. The resulting nanoparticles were larger than those used in the hamster ear study. The nanoparticles were prepared by dissolving (1) 400 mg of UK-157,147 and 1.2 g of ethyl cellulose in 9 ml of methylene chloride; and (2) 25 mg of NaGC in 20 ml of water. The two solutions were mixed and the nanoparticles were made using an emulsion procedure similar to the one described above, except that the 10-mg A/ml suspension was passed through a 0.2-μm filter.

2.3. Nanoparticle sizing

Nanoparticle size was measured by dynamic light scattering (DLS) using a BI-200SM nanoparticle size analyzer with a BI-9000AT correlator (Brookhaven Instruments Corp., Long Island, NY). Nanoparticle size is reported as the effective hydrodynamic diameter determined using the cumulant cubic algorithm. Size was typically measured in duplicate or triplicate and the average value reported. The width of the particle-size distribution is reported in terms of the polydispersity from the second cumulant.

Nanoparticle morphology and size heterogeneity was assessed using cryo-transmission electron microscopy (cryo-TEM) imaging. The solutions were sampled and prepared for cryo-TEM analysis using an FEI Vitrobot™ (FEI Company, Hillsboro, OR) and the following method. A 10-μl sample of solution was applied to a Lacey Carbon TEM grid in a Vitrobot chamber equilibrated to 90% relative humidity (RH). The grid was blotted once for 2 s and then immediately plunged into freezing liquid ethane. The grid was then transferred to a Taylor-Wharton liquid-nitrogen storage dewar until imaging could be performed. Imaging was carried out at 200 kV using a thermionic LaB6 electron source in the FEI Tecnai 20 Sphera TEM instrument using a Gatan Model 626 cryogenic holder (Gatan Inc., Pleasanton, CA) in the low-dose imaging mode facilitated by an FEI Tecnai user interface. The TEM instrument was equipped with a Gatan Multiscan CCD Model 794 camera, and images were captured using a Gatan digital micrograph.

The storage stability of two nanoparticle suspensions was tested: (1) the 1:3:2 UK-157,147:ethyl cellulose:NaGC/PMMA nanoparticles used in the *in vivo* tests to evaluate drug delivery to sebaceous glands; and (2) the 1:3:0.06 UK-157,147:ethyl cellulose:NaGC nanoparticles used for the hair-growth efficacy tests. Nanoparticles were stored as 10-mg A/ml suspensions for 3 months at room temperature, and particle sizes were measured by DLS. The suspensions were then filtered through a 0.2-μm syringe filter, and the UK-157,147 concentration was measured by high performance liquid chromatography (HPLC) analysis to test for aggregation of drug-containing particles into larger structures.

2.4. Nanoparticle suspension potency

The potency of the nanoparticle suspensions was measured to determine the total of encapsulated and dissolved drug. For this test, 50 μl of the nanoparticle suspension was diluted into 1 ml of acetonitrile to dissolve the nanoparticles. The drug concentration was then analyzed by HPLC using an Alltech Hypersil BDS C18 column (5 μm, 4.6 mm × 250 mm, 1 ml/min of 60:40 50-mM ammonium formate [pH 5]:acetonitrile; 20-μl injection volume; 25 °C column temperature; absorbance at 265 nm).

2.5. In vitro dissolution testing

The dissolution performance of the suspensions was evaluated as a function of nanoparticle concentration in a nonsink dissolution test. For this test, 1:3:2 UK-157,147:ethyl cellulose:NaGC/PMMA fluorescently labeled nanoparticles were manufactured as described above for those used in the hamster model. The total potency of the suspension was measured using the method described above.

The fraction of drug encapsulated in the nanoparticles was determined by subtracting the dissolved (i.e., unentrapped) drug from the total measured potency of the nanoparticle suspensions. The concentration of dissolved drug was measured by placing 250 μl of nanoparticle suspension in a microcentrifuge tube fitted with a 100-kDa MWCO filter, and centrifuging at 15,800 × *g* for 3 min to separate dissolved drug from drug entrapped in nanoparticles. Fifty microliters of the filtrate was diluted with 1 ml of acetonitrile and the drug concentration was analyzed by HPLC as described above. The fraction of drug entrapped in the nanoparticles was determined by subtracting the dissolved drug concentration from the total potency of the nanoparticle suspension. The analysis was performed in triplicate and the values were averaged.

The suspension was diluted to three concentrations – 18, 39, and 77 μgA/ml – and the rate and extent of dissolution was measured as a function of dilution into phosphate buffer solution (PBS) at pH 7.4. Diluted suspensions were placed in glass scintillation vials and stirred at 100 rpm using a magnetic stir bar. At each time point, duplicate 500-μl aliquots were removed from the vials, placed into

microcentrifuge tubes fitted with 100-kDa MWCO filters and spun at 15,800 × *g* for 3 min. After spinning, 100 μl of the filtrate was mixed with 500 μl of acetonitrile and analyzed by HPLC.

2.6. In vitro distribution in skin using a rabbit ear model

For this test, fresh rabbit ear tissue was used as a convenient model. The tissue was cut into pieces measuring approximately 1 cm × 1 cm, and the fur was trimmed to several millimeters in length. One hundred microliters of a suspension containing the 19:1:0.6 ethyl cellulose:MEH-PPV:NaGC fluorescently labeled nanoparticles described above (at a 30-mg/ml solids content) was applied to the tissue using a pipette. Tissue massage was not used to promote transport of nanoparticles into the follicles. The samples were incubated for 2 h in an ESPEC LH-113 temperature/humidity cabinet at 37 °C/50% RH (ESPEC Corp., Osaka, Japan). The tissue was then embedded in Tissue-Tek® OCT™ compound and microtomed into 5-μm-thick sections cut at −24 °C with a Leica 1850 cryostat. Sections were mounted on glass slides. Fluorescence imaging was performed with a Nikon Eclipse E600 microscope equipped with a Clemex LU11363-CLX camera and an epifluorescence filter block (G-2A) (excitation filter 510–560 nm, dichroic mirror 575 nm, emission filter 590 nm) with 2.0-s exposure time. The MEH-PPV excitation wavelength was 490 nm.

A 60:20:20 ethanol:propylene glycol:isopropyl myristate organic solution containing 1 mg/ml Nile Red was applied to rabbit ear tissue, as was an aqueous suspension containing 91-nm 10:0.1:0.17 ethyl cellulose:Nile Red:NaGC nanoparticles. Approximately 600 μl of solution or suspension was applied to 3 cm^2 of tissue, the tissue was massaged lightly for 10 s, and then equilibrated for 1 h at 40 °C/100% RH. The tissue was embedded in Tissue-Tek OCT compound for cryo-TEM analysis (sections were 5 μm, cut at −24 °C with a Leica 1310 Cryostat). Fluorescence imaging was performed using a Nikon Eclipse E600 microscope equipped with a Clemex LU11363-CLX camera and an epifluorescence filter block (G-2A) (excitation filter 510–560 nm, dichroic mirror 575 nm, emission filter 590 nm), with exposure times of 0.5 s for the solution and 1.0 s for the nanoparticle suspension. The Nile Red excitation wavelength was 460 nm.

2.7. In vivo delivery to sebaceous glands using a hamster ear model

For this test, three formulations were tested *in vivo* using a hamster ear model at 1% (w/v) UK-157,147:

(1) 60:20:20 alcohol:propylene glycol:isopropyl myristate (control);
(2) 1:3:2 UK-157,147:ethyl cellulose:NaGC/PMMA nanoparticles; and
(3) bulk crystals of UK-157,147.

Golden Syrian hamsters (body weight 110–115 g, supplied by Charles River) were anesthetized with isoflurane, transferred to a heated, temperature-controlled (37 °C) platform, and fitted with a nose-cone breathing apparatus that allowed controlled delivery of isoflurane to keep the animal moderately anesthetized to prevent movement. The animal and the chamber's heated platform were enclosed by a large Plexiglass™ cover.

A positive-displacement pipette was used to apply 20 μl of formulation to the ventral surface of an ear of the lightly anesthetized animal. Each formulation was applied to two ears, one left and one right from different animals, assigned randomly. The formulations were carefully spread over the central portion of the ear surface to minimize runoff. After 2 h, the animal was sacrificed and the ears were removed and carefully dissected to isolate the sebaceous glands (Niemiec et al., 1995).

The dissection procedure was as follows. The ears were cut off as close as possible to the skull and mounted, ventral side up, on a dissection board with pins. A Kimwipe® was used to dab excess formulation from the ear surface. The surface was stripped with transparent tape 25 times. Ears were cut along the body to separate the ventral and dorsal surfaces. The dermis on the ventral surface was peeled with forceps to reveal the follicle bulbs and sebaceous glands, which were scraped from the surface using 100 μl of HPLC-quality water. Scrapings were collected using Q-Tips®, which were placed in a container and extracted with 3.0 ml of a 50:50 acetonitrile:water solution by sonication for 30 min.

An aliquot from each vial was centrifuged for 10 min, and the supernatant was assayed for UK-157,147 by reverse-phase HPLC. HPLC was performed using an Agilent 1100 system, using a Luna C18(2) Phenomenex® reversed-phase column (3 μm, 100 Å, 150 mm × 4.6 mm) with a flow rate of 1.0 ml/min at ambient temperature. Detection was at 210 nm using an injection volume of 20.0 μl. The run time was 10 min. The mobile phase was 40:60 (v/v) acetonitrile:0.05 M ammonium formate at pH 5.0.

The results were analyzed using a two-sided Student's *t*-test to assess the significance of differences in uptake of drug from the two formulations.

2.8. Hair-growth efficacy using a C3H mouse model

Male C3H mice were used to assess hair growth. In this model (Hamada and Suzuki, 1996), the first few anagen (hair-growth) phases are synchronized, and the second telogen (resting-follicle) phase lasts for more than 4 weeks.

To assess the hair-growth effect of UK-157,147, various formulations containing 1% UK-157,417 were applied topically to the shaved lower back of age-matched male mice in the second telogen phase of the hair cycle. Ten animals per formulation were treated. Hair-growth was monitored by the onset of the anagen phase and grades of hair growth. The grades of hair growth were defined as 0 = no hair growth, 1 = initiation of hair growth, 2 = partial or sparse hair growth, and 3 = full hair growth. Twenty microliters of placebo vehicle or the various UK-157,417 formulations were applied twice daily, 5 days per week for 4 weeks, covering approximately 1 cm^2 on the shaved lower back. The hair growth was graded daily in the morning before dosing. After 4 weeks of dosing, the hair growth was monitored and graded daily for another week.

The *in vivo* experimental work reported in the present study was conducted under Institutional Animal Care and Use Committee (IACUC)-approved protocols and in compliance with the Guide for the Care and Use of Laboratory Animals (National Research Council, 2010).

3. Results

3.1. Nanoparticle size and entrapped drug

Because particle size can affect distribution of the nanoparticles when they are applied topically, particle diameters were determined by DLS for all formulations. Measurements were typically made in either duplicate or triplicate. In all cases, replicate measurements gave effective diameters that agreed to within <3%. DLS analysis showed that the diameters of the 19:1:0.6 ethyl cellulose:MEH-PPV:NaGC and 10:0.1:0.17 ethyl cellulose:Nile Red:NaGC nanoparticles used for the *in vitro* skin-distribution tests with rabbit ear tissue were 96 and 91 nm, respectively, with polydispersities of 0.18 and 0.10, respectively. The 1:3:2 UK-157,147:ethyl cellulose:NaGC/PMMA nanoparticles

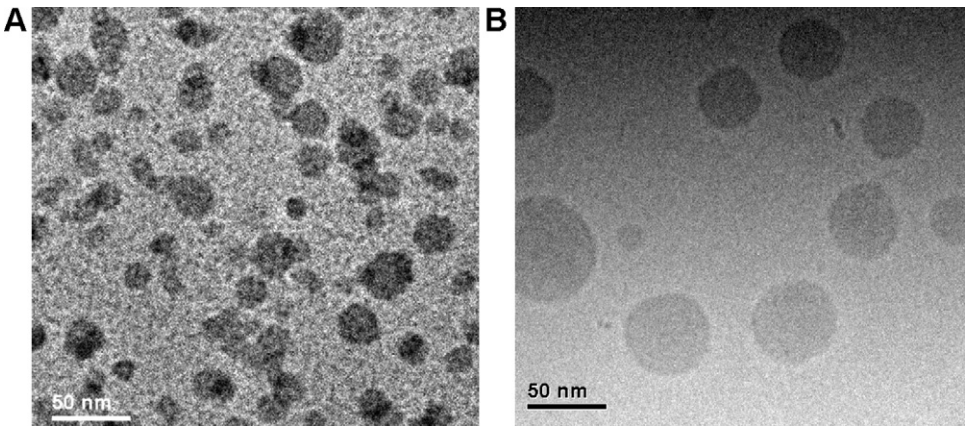

Fig. 2. Cryo-TEM image of 1:3:2 UK-157,147:ethyl cellulose:NaGC/PMMA (a) and 1:3:0.06 UK-157,147:ethyl cellulose:NaGC (b) nanoparticles.

used to evaluate drug delivery to sebaceous glands using the hamster ear model *in vivo* were 30 nm in diameter with a polydispersity of 0.14. The nanoparticle size was confirmed for formulations dosed *in vivo* using cryo-TEM imaging (Fig. 2). In previous studies, nanoparticle suspensions using this same formulation showed no change in size after storage at ambient temperature for 3 months.

Based on DLS measurements, the 1:3:0.06 UK-157,147:ethyl cellulose:NaGC nanoparticles dosed in the mouse efficacy model were 100 nm in diameter and had a polydispersity of 0.07. After storage for 3 months at room temperature at a concentration of 10 mg A/ml, these nanoparticles showed no significant change in size (diameter of 100 nm, polydispersity of 0.05) and little loss in potency (9.8 mg A/ml) after filtration through a membrane with a nominal pore size of 0.2 μm. These results confirm that no significant aggregation of nanoparticles into larger structures occurred during storage.

The total potency of the 1:3:2 UK-157,147:ethyl cellulose:NaGC/PMMA nanoparticles was 12.9 mg A/ml, whereas the dissolved drug measured by centrifuging the suspension through 100-kDa MWCO filters was 1.29 mg A/ml, resulting in an encapsulated fraction of 90%. The encapsulated fraction varies with nanoparticle concentration, as described in the partitioning model described below.

3.2. *In vitro* distribution within the skin using rabbit ear tissue

A fluorescently labeled placebo suspension containing 19:1:0.6 ethyl cellulose:MEH-PPV:NaGC nanoparticles was applied *in vitro* to rabbit ear tissue as described above to qualitatively assess the penetration of nanoparticles into the follicles. Fig. 3 shows representative bright-field and fluorescent images obtained after incubation of the samples for 2 h at 37 °C/50% RH. As the figure shows, substantial fluorescence was observed on the surface of the stratum corneum, as expected. However, the image also clearly shows delivery of nanoparticles to the hair follicles, with little or no fluorescence observed elsewhere in the epidermal or dermal layers.

To assess the ability of an aqueous nanoparticle suspension to limit the distribution of drug to the bulk dermal tissue (and, therefore, to the systemic circulation), placebo nanoparticles containing Nile Red, a poorly water-soluble lipophilic dye were prepared. The dye was used as a model of a small-molecule low-solubility drug that could typically be delivered topically using an organic solution. The nanoparticles containing the Nile Red dye were dosed as a suspension to rabbit ear tissue *in vitro*, and the tissue samples were sectioned for imaging. An organic solution containing Nile Red was likewise dosed as a control.

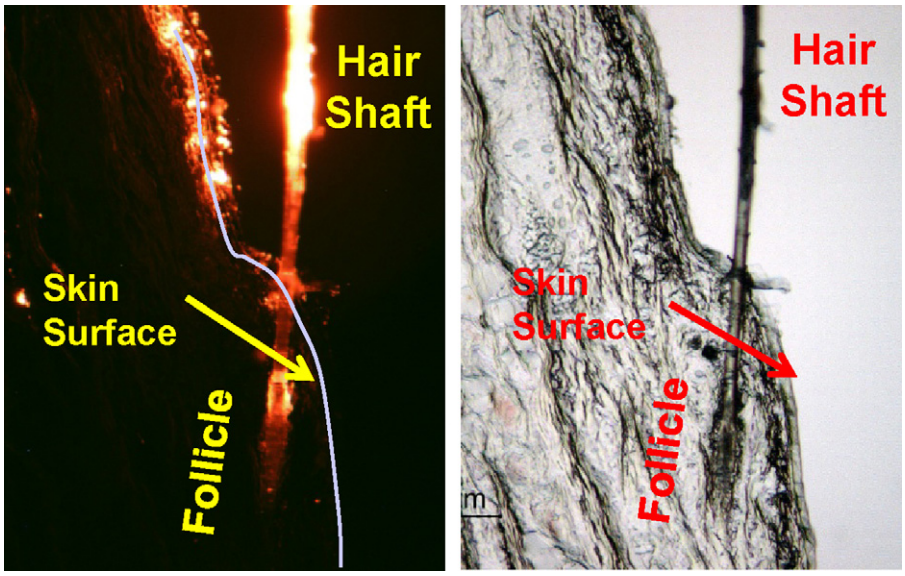

Fig. 3. Fluorescent (left) and bright-field (right) microscopy images of rabbit ear tissue incubated for 2 h with 19:1:0.6 ethyl cellulose:MEH-PPV:NaGC fluorescent nanoparticles.

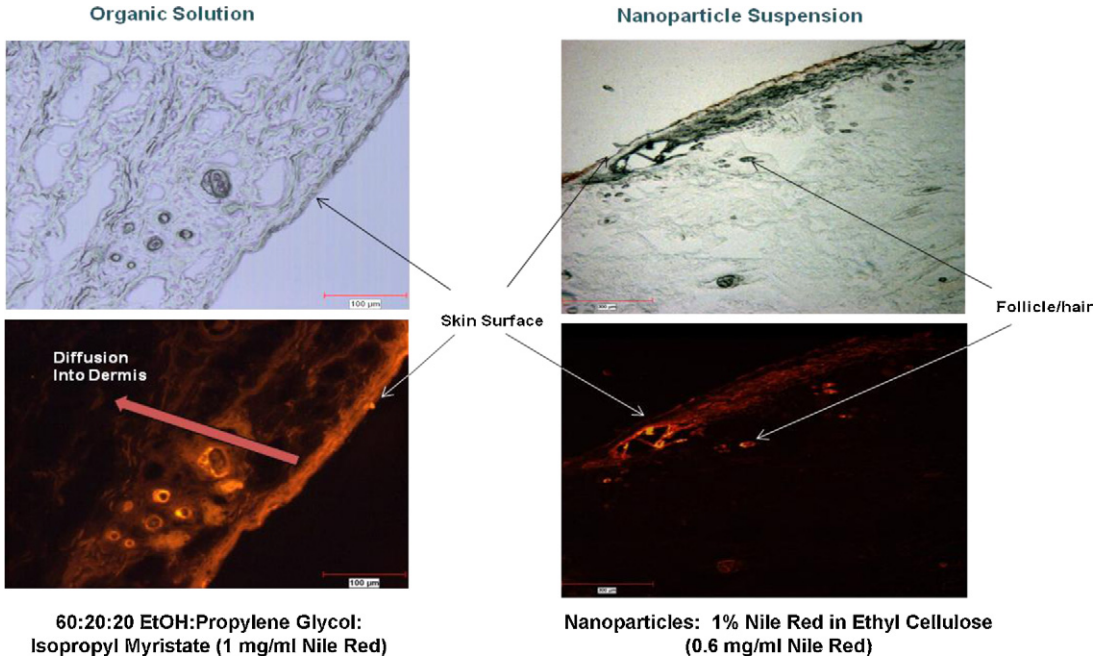

Fig. 4. Rabbit ear tissue dosed with 60% EtOH:20% propylene glycol:20% isopropyl myristate (1 mg/ml Nile Red) (left), and 10:0.1:0.17 ethyl cellulose:Nile Red:NaGC nanoparticles (right).

The bright-field and fluorescent images in Fig. 4 show the distribution of Nile Red dye within the tissue for the nanoparticles and the organic solution. As the figure shows, the dye from the nanoparticle formulation is located almost exclusively on the skin surface and in the hair follicle. In contrast, results for the organic solution—which represents a type typically used for topical drug delivery—show substantial amounts of dye distributed throughout the skin layers.

3.3. Drug delivery to sebaceous glands using a hamster ear model

A suspension containing 1:3:2 UK-157,147:ethyl cellulose:NaGC/PMMA nanoparticles (10 mg A/ml or 1% w/v) was dosed to hamster ears, and the concentration of UK-157,147 in the sebaceous glands was measured at 1- and 2-h time points, as described above. The concentrations were compared with those measured after application of a similar amount of UK-157,147 in a 60:20:20 ethanol:propylene glycol:isopropyl myristate solution. A third formulation, consisting of bulk crystals of UK-157,147 in 20 mg/ml NaGC, was also tested.

Fig. 5 shows the concentrations of UK-157,147 in the glands at the 2-h time point. As the figure shows, comparable amounts of drug were delivered using the nanoparticle suspension and the organic solution, even though the amount of dissolved drug was much different. The differences in uptake did not meet the $P < 0.05$ criterion for significance. Conversely, the amount of drug delivered by the bulk crystalline suspension was much less than for the other two formulations.

3.4. Efficacy in a C3H mouse model

In a previous study (unpublished data), we demonstrated that UK-157,147 in 70:30 ethanol:propylene glycol formulation (w/v) stimulated hair growth in the C3H mouse model. In this study, we used 1% UK-157,147 in a 70:30 ethanol:propylene glycol formulation as a positive control. This study showed that hair growth was stimulated by a suspension containing 1:3:0.06 UK-157,147:ethyl cellulose:NaGC nanoparticles. As shown in Fig. 6, the efficacy of UK-157,147 in the nanoparticle suspension was comparable to that of the ethanol:propylene glycol formulation. The onset of hair growth

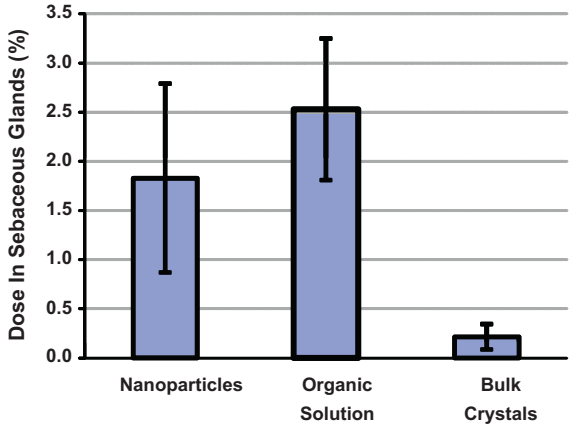

Fig. 5. Dose recovered from sebaceous glands of hamster ears for three UK-157,147 formulations.

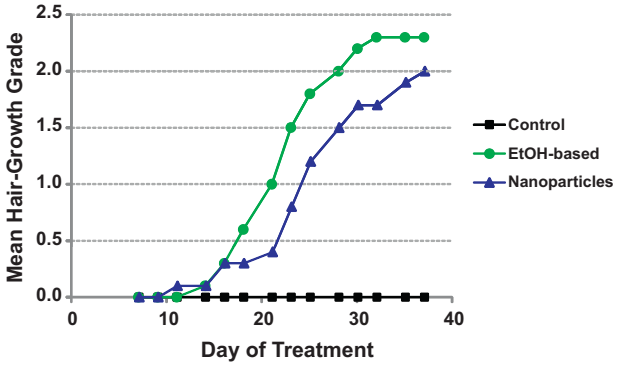

Fig. 6. Effect of 1% UK-157,147 formulated in a nanoparticle suspension or an organic solution on hair growth (1:3:0.06 UK-157,147:ethyl cellulose:NaGC nanoparticles).

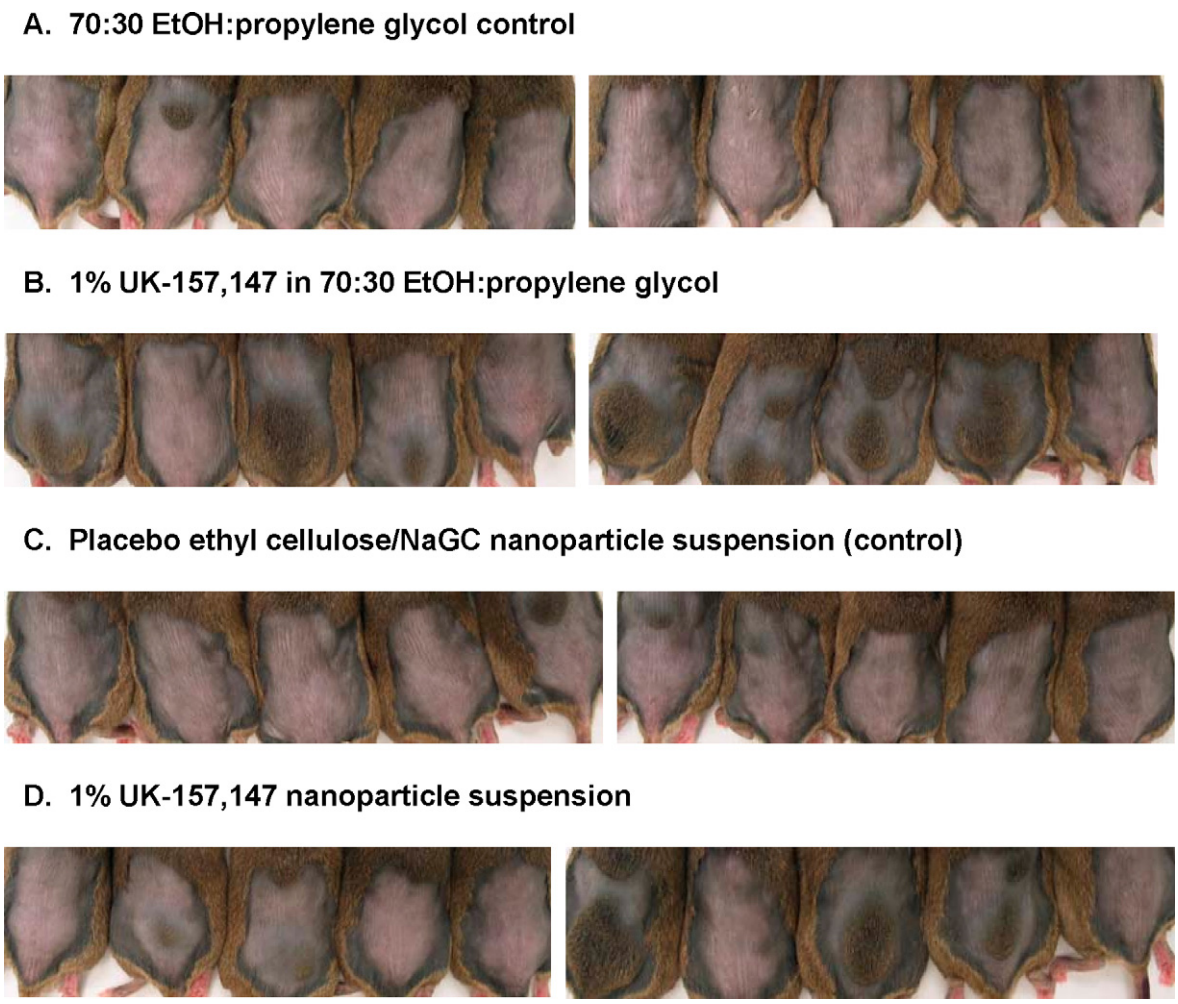

Fig. 7. Photographic images of mice treatment with a solution control (A), UK-157,147 solution (B), placebo nanoparticle suspension control (C) and UK-157,147 nanoparticle suspension (D).

occurred at similar times for the two formulations. The vehicle controls in the study did not stimulate hair growth.

Fig. 7 shows photographs of the hair growth in mice on day 25 of the study. Fifty percent of the mice treated with the 1% UK-157,147 nanoparticle suspension had visible hair growth on the lower back areas, whereas 70% of the mice treated with 1% UK-157,147 ethanol/propylene glycol had hair growth. At end of the study (day 35), hair growth was observed for 70% of the mice treated with the 1% UK-157,147 nanoparticle suspension and 80% of the mice treated with 1% UK-157,147 ethanol/propylene glycol. The mice treated with control vehicles had no hair growth in the treated areas.

3.5. Dissolution testing

The dissolution performance of 1:3:2 UK-157,147:ethyl cellulose:NaGC/PMMA nanoparticles was tested using various nanoparticle concentrations in PBS at pH 7.4. As shown in Fig. 8, the active concentration in PBS reached a constant value within 5 min and the extent of dissolution increased monotonically with decreasing nanoparticle concentration.

4. Discussion

The size of the nanoparticles made using NaGC can be adjusted by varying the concentration of NaGC, with higher NaGC concentrations resulting in smaller nanoparticles. This is likely because larger amounts of surfactant stabilize the larger surface area associated with the smaller emulsion droplets used to make the nanoparticles. In addition, the surfactant helps stabilize the solid nanoparticles to prevent aggregation in suspension once they are formed.

In tests with the hamster ear model, a relatively high level of NaGC (333 mg/g solids) was used to make the smallest nanoparticles possible (30 nm in diameter). This was done based on the hypothesis that smaller nanoparticles would penetrate the follicle and sebaceous glands more easily than larger nanoparticles.

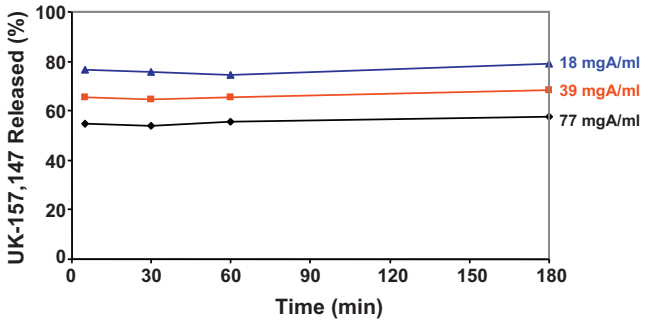

Fig. 8. Dissolution results for 1:3:2 UK-157,147:ethyl cellulose:NaGC/PMMA nanoparticles dosed at 18, 39, and 77 μgA/ml in PBS at pH 7.4.

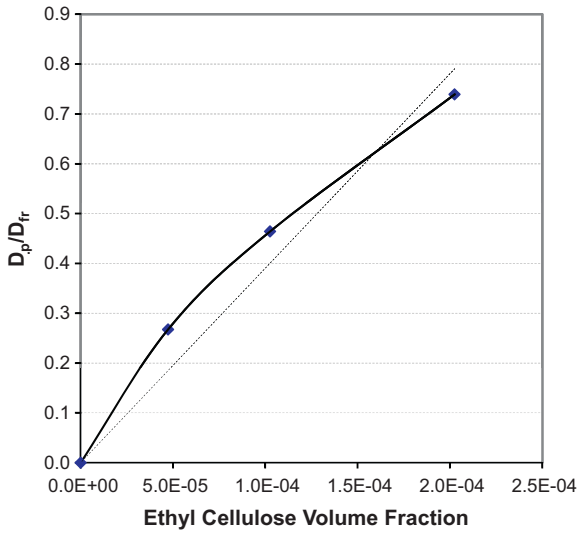

Fig. 9. Plot of the ratio of drug mass in polymer to dissolved drug mass versus ethyl cellulose volume fraction measured for 1:3:2 UK-157,147:ethyl cellulose:NaGC/PMMA nanoparticles in nonsink dissolution testing.

For tests with the mouse model, we sought to avoid use of large amounts of surfactant because the nanoparticles would be dosed over a longer treatment period. The lower NaGC concentrations (15 mg/g solids) used for the nanoparticles in these tests resulted in larger (100 nm diameter) nanoparticles. More work would be required to assess the effect of nanoparticle size on penetration into the sebaceous glands in the hamster model and hair-growth efficacy in the mouse model.

During nonsink dissolution testing of the nanoparticles (Fig. 8), after dilution in the dissolution medium, the concentration of free drug essentially reached its steady-state value by the first time point (i.e., at 5 min). The fraction of drug released in the test was inversely related to the nanoparticle concentration. The rapid dissolution is due to the short diffusion distance of drug from inside the nanoparticle core to its surface. The rapid release from the nanoparticles to reach a concentration that is in equilibrium with the active remaining in the nanoparticles indicates that the drug is not kinetically trapped within the polymeric matrix of the nanoparticle but resides within the nanoparticle due to a high thermodynamic solubility. The dissolution data suggest that thermodynamic partitioning of the drug occurs between the core of the nanoparticle and the aqueous medium.

The partition coefficient can be calculated by comparing the ratio of drug in the polymeric nanoparticle to dissolved (free) drug at steady state using

$$\frac{D_p}{D_{fr}} = K_p V_p,$$

where D_p is drug in the nanoparticle, D_{fr} is dissolved "free" drug, K_p is the polymer/aqueous partition coefficient, and V_p is the volume fraction of ethyl cellulose in the suspension.

Fig. 9 plots the ratio of drug in the nanoparticle to the drug dissolved in the aqueous solution as a function of ethyl cellulose volume fraction for a given drug loading at several total drug concentrations. The partitioning model is validated by the approximate linearity of the plot (dashed line). An average partition coefficient of 3900 can be calculated from a linear fit to the data and suggests a solubility of UK-157,147 in ethyl cellulose of approximately 50 wt.% (assuming an ethyl cellulose density of 1.14 g/ml). Therefore, UK-157,147 is supersaturated in the core of the nanoparticle for all loadings greater than 50 wt.%. The slight curvature of the line plotted in Fig. 9 suggests that as drug loading increases, the partition coefficient into the ethyl cellulose core decreases.

Based on this analysis, for drug loadings lower than about 50 wt.% in ethyl cellulose, the activity of drug in the nanoparticles and the corresponding free-drug concentration in aqueous solution is less than the crystalline solubility. These low-activity nanoparticles can be advantageous for follicular delivery in that they provide small, rapidly sourcing drug carriers that can effectively penetrate the follicles and act as a depot, but do not provide high activity in terms of dissolved drug concentration that will drive drug into the rest of the skin tissue from the follicles.

The *in vitro* imaging of rabbit ear tissue dosed with fluorescent nanoparticles clearly shows the potential advantage of the nanoparticles for targeted delivery to the follicles, limiting adverse events due to systemic exposure and, thereby, raising the therapeutic index. The images in Figs. 3 and 4 suggest minimal exposure to the dermis for the nanoparticles and their cargo, the lipophilic dye Nile Red, which is a reasonable model for a low-solubility lipophilic small-molecule drug. As the images show, during this 2-h exposure time, nanoparticle distribution is limited to the surface of the skin and the follicles, because the 100-nm nanoparticles are too large to penetrate the stratum corneum.

Likewise, the lipophilic Nile Red cargo does not appreciably distribute throughout the skin from the aqueous nanoparticle suspension during the 2-h exposure. Its distribution is also limited largely to the top surface of the skin and the hair follicle. Conversely, when administered using a typical organic vehicle for topical drug delivery, the dye shows significant penetration throughout the epidermal and dermal layers of the skin during the 2-h experiment. This is due to the large permeation-enhancing capability of the organic solution from a variety of mechanisms, including disruption of the barrier layer of skin and the solvent's ability to carry drug with it into the skin as it penetrates (Williams and Barry, 2004).

Hamster ear models are commonly used to evaluate the effect of drug on sebaceous glands as well as follicular drug delivery after topical applications (Plewig and Luderschmidt, 1977; Lieb et al., 1994). As shown in Fig. 5, the relative amount of UK-157,147 in sebaceous glands are aqueous (bulk crystal) suspension < aqueous nanoparticles < ethanol/propylene glycol/isopropyl myristate solution. It is known that the delivery of the compound is more efficient from the ethanol-based solution, because this organic vehicle enhances permeation through transepidermal and transfollicular pathways, producing higher drug concentrations in local tissues and, consequently, higher systemic exposure.

Interestingly, compared with an aqueous (bulk crystal) suspension, the aqueous nanoparticle suspension produced a substantially higher drug concentration in the sebaceous glands, indicating the predominance of transfollicular delivery over transepidermal delivery. In a previous study using liposomal formulation for topical administration, Lieb et al. (1994) showed that the ratio of local efficacy versus systemic efficacy was higher from a liposomal formulation than from 50% ethanol, possibly reflecting reduced systemic exposure from the nanoparticle formulation. Similar to liposomes the nanoparticle formulation reduced drug systemic exposure even though the drug concentration in sebaceous glands was comparable to that obtained using an ethanol solution.

Drug deposition in sebaceous glands appears to correlate well with efficacy, as shown in Figs. 3 and 4. The hair growth from the nanoparticles was significantly faster than from the aqueous vehicle control, even though it was slightly slower than from the ethanol-based solution. Based on these results, nanoparticle suspensions offer an attractive alternative to organic solutions, especially for drugs with a low therapeutic index due to systemic toxicity.

5. Conclusions

Based on the results of these studies, an aqueous nanoparticle suspension can be used to deliver UK-157,147 to the sebaceous glands in a hamster ear model. Similar formulations also stimulated hair growth in the C3H mouse model, caused no visible skin irritation, and were well-tolerated. *In vitro* imaging of rabbit ear tissue suggested that aqueous nanoparticle suspensions can limit distribution of small-molecule drugs to the dermis while delivering drug to the follicles.

In aggregate, these results support the idea that nanoparticle suspensions can effectively deliver low-molecular-weight active pharmaceutical ingredients to hair follicles through the transfollicular route, while limiting distribution to the rest of the skin and to systemic circulation. By targeting delivery to the hair follicles, nanoparticles have the potential to improve the therapeutic index for a number of topically applied drugs.

Acknowledgements

The authors would like to thank Dr. Philip Nixon for reviewing the manuscript, and Dr. Dwayne Friesen, Gary Ewing, and David Pole for valuable discussions.

References

Alvarez-Roman, R., Naik, A., Kalia, Y.N., Guy, R.H., Fessi, H., 2004. Skin penetration and distribution of polymeric nanoparticles. J. Control. Release 99, 53–62.

Chen, H., Chang, X., Du, D., Liu, W., Liu, J., Weng, T., Yang, Y., Xu, H., Yang, X., 2006. Podophyllotoxin-loaded solid lipid nanoparticles for epidermal targeting. J. Control. Release 110, 296–306.

Chourasia, R., Jain, S.K., 2009. Drug targeting through pilosebaceous route. Curr. Drug Targets 10, 950–967.

Hamada, K., Suzuki, K., 1996. Evaluation of biochemical indices as a hair cycle marker in C3H mice. Exp. Anim. 45, 251–256.

Jung, S., Otberg, N., Thiede, G., Richter, H., Sterry, W., Panzner, S., Lademann, J., 2006. Innovative liposomes as a transfollicular drug delivery system: penetration into porcine hair follicles. J. Invest. Dermatol. 126, 1728–1732.

Knorr, F., Lademann, J., Patzelt, A., Sterry, W., Blume-Peytavi, U., Vogt, A., 2009. Follicular transport route – research progress and future perspectives. Eur. J. Pharm. Biopharm. 71, 173–180.

Lademann, J., Otberg, N., Jacobi, U., Hoffman, R., Blume-Peytavi, U., 2005. Follicular penetration and targeting. J. Invest. Dermatol. Symp. Proc. 10, 301–303.

Lademann, J., Richter, H., Teichmann, A., Otberg, N., Blume-Peytavi, U., Luengo, J., Weib, B., Schaefer, U.F., Lehr, C.M., Wepf, R., Sterry, W., 2007. Nanoparticles—an efficient carrier for drug delivery into the hair follicles. Eur. J. Pharm. Biopharm. 66, 159–164.

Lekki, J., Stachura, Z., Dabroś, W., Stachura, J., Menzel, F., Reinert, T., Butz, T., Pallon, J., Gontier, E., Ynsa, M.D., Moretto, P., Kertesz, Z., Szikszai, Z., Kiss, A.Z., 2007. On the follicular pathway of percutaneous uptake of nanoparticles: ion microscopy and autoradiography studies. Nucl. Instrum. Method Phys. Res. B 260, 174–177.

Lieb, L., Flynn, G., Weiner, N., 1994. Follicular (pilosebaceous unit) deposition and pharmacological behavior of cimetidine as a function of formulation. Pharm. Res. 11, 1419–1423.

Mahe, B., Vogt, A., Liard, C., Duffy, D., Abadie, V., Bonduelle, O., Boissonnas, A., Sterry, W., Verrier, B., Blume-Peytavi, U., Combadiere, B., 2009. Nanoparticle-based targeting of vaccine compounds to skin antigen-presenting cells by hair follicles and their transport in mice. J. Invest. Dermatol. 129, 1156–1164.

Moghimi, S.M., Hunter, A.C., Murray, J.C., 2001. Long-circulating and target-specific nanoparticles: theory to practice. Pharmacol. Rev. 53, 284–318.

National Research Council, 2010. Guide for the Care and Use of Laboratory Animals. National Academies Press, Washington, DC.

Niemiec, S.M., Ramachandran, C., Weiner, N., 1995. Influence of nonionic liposomal composition on topical delivery of peptide drug into pilosebaceous units: an in vivo study using the hamster ear model. Pharm. Res. 12, 1184–1188.

Otberg, N., Patzelt, A., Rasulev, U., Hagemeister, T., Linscheid, M., Sinkgraven, R., Sterry, W., Lademann, J., 2008. The role of hair follicles in the percutaneous absorption of caffeine. Br. J. Clin. Pharmacol. 65, 488–492.

Plewig, G., Luderschmidt, C., 1977. Hamster ear model for sebaceous glands. J. Invest. Dermatol. 68, 171–176.

Rancan, F., Papakostas, D., Hadam, S., Hackbarth, S., Delair, T., Primard, C., Verrier, B., Sterry, U., Blume-Peytavi, U., Vogt, A., 2009. Investigation of polylactic acid (PLA) nanoparticles as drug delivery systems for local dermatotherapy. Pharm. Res. 26, 2027–2036.

Rolland, A., Wagner, N., Chatelus, A., Shroot, B., Schaefer, H., 1993. Site-specific drug delivery to pilosebaceous structures using polymeric microspheres. Pharm. Res. 10, 1738–1744.

Shim, J., Seok Kang, H., Park, W.S., Han, S.H., Kim, J., Chang, I.S., 2004. Transdermal delivery of monoxidil with block copolymer nanoparticles. J. Control. Release 97, 477–484.

Singh, R., Lillard Jr., J.W., 2009. Nanoparticle-based targeted drug delivery. Exp. Mol. Pathol. 86, 215–223.

Tsujimoto, H., Hara, K., Tsukada, Y., Huang, C.C., Kawashima, Y., Arakaki, M., Okayasu, H., Mimura, H., Miwa, N., 2007. Evaluation of the permeability of hair growing ingredient encapsulated PLGA nanospheres to hair follicles and their hair growing effects. Bioorg. Med. Chem. Lett. 17, 4771–4777.

Vogt, A., Combadiere, B., Hadam, S., Stieler, K.M., Lademann, J., Schaefer, H., Autran, B., Sterry, W., Blume-Peytav, U., 2006. 40 nm, but not 750 or 1500 nm, nanoparticles enter epidermal CD1a+ cells after transcutaneous application on human skin. J. Invest. Dermatol. 126, 1316–1322.

Williams, A., Barry, B., 2004. Penetration enhancers. Adv. Drug Deliv. Rev. 56, 603–618.

Wu, X., Price, G.J., Guy, R.H., 2009. Disposition of nanoparticles and an associated lipophilic permeant following topical application to the skin. Mol. Pharm. 6, 1441–1448.

Yih, T.C., Al-Fandi, M., 2006. Engineered nanoparticles as precise drug delivery systems. J. Cell. Biochem. 97, 1184–1190.